



Techno-economic analysis of calcium looping processes for low CO₂ emission cement plants



Edoardo De Lena^a, Maurizio Spinelli^b, Manuele Gatti^{a,b}, Roberto Scaccabarozzi^{a,b}, Stefano Campanari^a, Stefano Consonni^{a,b}, Giovanni Cinti^c, Matteo C. Romano^{a,*}

^a Politecnico di Milano, Department of Energy, via Lambruschini 4, 20156 Milan, Italy

^b Laboratorio Energia & Ambiente Piacenza (LEAP), via Nino Bixio 27/C, 29121 Piacenza, Italy

^c Italcementi, HeidelbergCement Group, via Tridentina 1, 24100 Bergamo, Italy

ARTICLE INFO

Keywords:

Cement
Ca-Looping
CO₂ capture
Economic analysis
Retrofitting

ABSTRACT

The scope of this work is to perform a techno-economic analysis of two Calcium Looping processes (CaL) for CO₂ capture in cement plants. Both tail-end CaL system with fluidized bed reactors and integrated CaL system with entrained flow reactors have been considered in the analysis. The calculation of the heat and mass balances and the economic analysis are consistent with the methodology defined in the framework of the H2020 Cemcap project.

The analysis shows that the assessed CaL systems (especially the tail-end configuration) involve a significant increase of fuel consumption compared to a reference cement kiln without carbon capture. However, a large part of this additional energy input is exploited in a heat recovery steam cycle, which generates the electric power required to satisfy the consumption of the CO₂ capture auxiliaries (i.e. the power absorbed by the air separation and CO₂ compression and purification units). The integrated CaL process features a lower rise of equivalent fuel consumption (+59% compared to the reference) and a larger reduction of direct CO₂ emission (-93% compared to the reference). The specific primary energy consumption for CO₂ avoided (SPEC_{CA}), which takes into account also the indirect fuel consumption/savings and indirect emissions/avoided emissions due to electricity exchange (import/export) with the grid, ranges between 3.17–3.27 MJ_{LHV}/kg_{CO2} for the integrated system vs. 3.76–4.42 MJ_{LHV}/kg_{CO2} for tail-end cases, depending on the scenario considered for the grid electricity mix.

The economic analysis highlights that CaL processes are capital intensive, which involve, roughly, a doubling of the Capex of the whole cement plant with CCS compared to a greenfield conventional cement plant. However, the obtained cost of CO₂ avoided is competitive with alternative technologies and ranges between about 52 €/t_{CO2} of the tail-end configuration and 58.6 €/t_{CO2} of the integrated one.

1. Introduction

Cement production is responsible for about 8% of global anthropogenic CO₂ emissions (Olivier et al., 2016). In state-of-the-art dry clinker burning processes, CO₂ produced from CaCO₃ calcination represents about 60% of the total CO₂ emissions, the remaining fraction being emitted from fuel combustion. In the framework of the H2020 CEMCAP project (CEMCAP, 2015), different technologies for CO₂ capture in cement plants have been assessed and benchmarked, namely oxyfuel combustion, chilled ammonia, membrane-assisted CO₂ liquefaction and Calcium Looping (CaL).

CaL can be integrated in a cement kiln through two fundamental approaches. The first one is the tail-end process configuration, where

the CaL CO₂ capture process is placed downstream the clinker burning line and the carbonator treats the flue gas exiting the cement kiln as an end-of-pipe process (Atsonios et al., 2015; De Lena et al., 2017; Ozcan et al., 2013). In this integration approach, the CaL system is based on circulating fluidized bed reactors, with an operating principle successfully proven up to 1.7 MW_{th}-scale (Arias et al., 2013; Kremer et al., 2013) for CO₂ capture from coal-fired power plants flue gas and more recently demonstrated experimentally at 30 kW_{th} and 200 kW_{th} scale on flue gases with higher CO₂ concentration, representative of cement kiln effluents (Arias et al., 2017a; Hornberger et al., 2017). A comprehensive process integration study with an extensive sensitivity analysis was also recently published by the same working group of this paper (De Lena et al., 2017), which showed the potential of this process in

* Corresponding author.

E-mail address: matteo.romano@polimi.it (M.C. Romano).

<https://doi.org/10.1016/j.ijggc.2019.01.005>

Received 3 October 2018; Received in revised form 4 January 2019; Accepted 4 January 2019

1750-5836/© 2019 The Authors. Published by Elsevier Ltd. This is an open access article under the CC BY-NC-ND license (<http://creativecommons.org/licenses/by-nc-nd/4.0/>).

| Nomenclature | |
|-----------------------|--|
| <i>Acronyms</i> | |
| ASU | Air separation unit |
| CaL | Calcium looping |
| Capex | Capital expenditure |
| CCA | Cost of CO ₂ avoided |
| CCS | Carbon Capture and Storage |
| CF _{process} | Process contingency factor |
| CF _{project} | Project contingency factor |
| CHP | Combined heat and power |
| COC | Cost of cement |
| CPU | CO ₂ purification unit |
| EC | Equipment cost |
| ECO | Economizer |
| EVA | Evaporator |
| HT | High temperature |
| IC | Installation cost |
| IL | Integration level |
| INCF | Indirect cost factor |
| LHV | Lower heating value |
| LT | Low temperature |
| OCF | Owner's cost factor |
| Opex | Operating expenditure |
| PoE | Price of electricity |
| PoF | Price of fuel |
| SH | Superheater |
| SPECCA | Specific primary energy for CO ₂ avoided [MJ _{LHV} /kg _{CO2}] |
| TDC | Total direct cost |
| TPC | Total plant cost |
| TRL | Technology readiness level |
| TSA | Temperature swing adsorption beds |
| USC | Ultra supercritical |
| <i>Symbols</i> | |
| e_{CO_2} | Direct CO ₂ emissions from the cement plant [kg/s or kg/t] |
| $e_{CO_2,e}$ | Indirect CO ₂ emissions associated to power consumption [kg/s or kg/t or kg/MWh] |
| $e_{CO_2,eq}$ | Equivalent CO ₂ emissions of the cement plant [kg/s or kg/t] |
| $E_{CO_2,e}$ | Specific CO ₂ emissions associated to power generation [kg/s or kg/t or kg/MWh] |
| F_0 | Molar flow of CaCO ₃ in the preheated raw meal entering the calciner [kmol/s] |
| F_{Ca} | Sorbent molar flow from the calciner to the carbonator [kmol/s] |
| \bar{F}_{CO_2} | Molar flow of CO ₂ entering the carbonator [kmol/s] |
| \dot{m} | Mass flow rate [kg/s or tpd] |
| P_e | Electric power [MW _e or MWh _e /t _{clk}] |
| q | Direct fuel consumption in the cement plant [MW _{LHV} or MJ _{LHV} /kg _{clk}] |
| q_e | Indirect fuel consumption associated to power consumption [MW _{LHV} or MJ _{LHV} /kg _{clk}] |
| q_{eq} | Equivalent fuel consumption of the cement plant [MW _{LHV} or MJ _{LHV} /kg _{clk}] |
| X_{max} | Sorbent conversion degree after the fast kinetically controlled period [-] |
| <i>Greek letters</i> | |
| η_e | Electric efficiency |
| <i>Subscripts</i> | |
| cem | Cement |
| clk | Clinker |
| e | Electric |
| eq | Equivalent |
| ref | Reference plant without CO ₂ capture |
| th | Thermal |

achieving high CO₂ capture efficiency and technical retrofittability of existing cement kilns.

The second option is the integrated CaL process configuration, where the carbonator is integrated in the preheater of the clinker burning line and treats only the flue gas from the rotary kiln and the oxyfuel CaL calciner coincides with the cement kiln precalciner (Marchi et al., 2012a, 2012b; Rodríguez et al., 2012; Romano et al., 2014). In the integrated CaL configuration, two fundamental differences can be highlighted with respect to the tail-end CaL configuration: (i) calcined raw meal (i.e. CaO with other SiO₂, Al₂O₃ and Fe₂O₃ raw constituents) is preferably used as a source of CaO sorbent for the carbonator rather than pure limestone; (ii) because of the small particle size of the raw meal ($d_{50} = 10\text{--}20\ \mu\text{m}$), cement raw meal falls in the region of cohesive particles (Geldart C particles (Geldart, 1973)) and entrained-flow reactors operating in the dilute pneumatic transport regime are preferable over fluidized beds. Recent research on the integrated CaL configuration for cement plants involved the assessment of the properties of the raw meal as CO₂ sorbent in TGA and drop tube reactors (Alonso et al., 2017; Pathi et al., 2013; Turrado et al., 2018) and the modelling of the entrained-flow carbonator (Spinelli et al., 2018).

An overview of the technical pros and cons of the two CaL integration approaches is available in recent works (De Lena et al., 2017; Spinelli et al., 2018, 2017).

This work aims at assessing the performance and costs of the two alternative CaL configurations for CO₂ capture in cement plants, under

the framework of technical and economic assumptions described by Anantharaman et al. (2017), enabling fair comparison with competing technologies, such as MEA scrubbing, oxyfuel, chilled ammonia and membranes.

Results presented in this work are based on: (i) validated cement kiln model (Campanari et al., 2016); (ii) latest entrained-flow carbonator model for the integrated CaL process (Spinelli et al., 2018); (iii) accurate design of the heat recovery steam cycle, with realistic steam parameters and turbine efficiency for the size of the plant; (iv) equipment sizing and capital cost estimation methodologies supported by industrial experience and (v) shared methodology for performance evaluation and economic analysis (Anantharaman et al., 2017).

This paper is structured as follows: Section 2 presents the two CaL concepts investigated and describes the process integration both with the cement kiln and with the heat recovery cycle with the support of Process Flow Diagrams and Temperature-Heat Duty diagrams; Section 3.1 reports the methodology followed for process simulation and the main assumptions for the energy performance assessment, whose results are then discussed in Section 3.2; Section 4.1 illustrates the economic framework also providing details on the equipment cost functions as well as on the assumptions for Capex and Opex calculations, while Section 4.2 discloses the economic results and presents the outcome of a sensitivity analysis on the most significant economic parameters; finally, in Section 5 conclusions are drawn.

2. Calcium-Looping cement plants

2.1. Tail-end calcium looping

A schematic of the cement kiln with CO₂ capture by the tail-end CaL process is shown in Fig. 1. Flue gas from the preheater (stream #18) are compressed by a fan and fed to the fluidized bed carbonator, where CO₂ is captured by means of the reaction with CaO-rich sorbent (#24). CO₂-lean gas (#20) exit the carbonator at 650 °C, are partly cooled and used as drying agent in the raw mill. Carbonated sorbent produced in the carbonator (#22) is regenerated by oxyfuel combustion calcination in the fluidized bed calciner. Oxygen produced in the air separation unit (#5) is preheated and mixed with recirculated CO₂-rich gas (#13) to achieve O₂ concentration of 50% before entering the calciner (#9). CO₂-rich gas released by the calciner at 920 °C is cooled down to 400 °C and partly recirculated to the calciner (#13). The remaining gas fraction is further cooled and sent to the CO₂ purification unit (CPU), where CO₂ is purified to a molar concentration higher than 95%, according to specifications for pipeline CO₂ transport (Anantharaman et al., 2017; NETL, 2012).

Part of the calcined solids from the CaL calciner is extracted from the loop (#2), cooled, mixed with the remaining portion of the raw meal fed to the cement kiln and milled in the raw mill to an average particle size of 10–20 μm. A fraction of the sorbent material is continuously purged from the CaL process to avoid excessive build-up of inert species (i.e. coal ash and CaSO₄) in the solids, that reduce the average activity of the solids for CO₂ capture. Therefore, the purge of

the CaL process needs to be compensated with a limestone make-up (#8), which is first sent to a dedicated limestone mill where it is crushed to the particle size suitable for fast fluidized beds (i.e. average size of 100–300 μm). The integration level (IL) (Eq.(1)) is defined as the ratio between the limestone fed to the CaL process through the limestone mill (#8) and the total amount of CaCO₃ fed to the cement kiln (through streams #8 and #1). As pointed out in the results section and extensively discussed in (De Lena et al., 2017), IL significantly affects the heat input to the CaL calciner and the overall energy balance of the plant.

$$IL = \frac{\text{CaCO}_3 \text{ fed to the CaL process}}{\text{Total CaCO}_3 \text{ fed to the plant}} \quad (1)$$

A steam cycle is needed to recover the large thermal power generated in the CaL process (Fig. 2). Most of the thermal power is recovered from the cooled carbonator and the CO₂-rich gas released from the calciner. A non-reheated steam cycle with evaporation pressure of 100 bar and SH temperature of 530 °C have been assumed, compatible with the resulting steam cycle size (Anantharaman et al., 2017; Consonni and Viganò, 2012), which is characterized by a steam turbine gross power output between 40 and 66 MW for IL of 50% and 20% respectively.

For a detailed discussion on the tail-end CaL plant configuration, on thermal integration between the CaL system and the steam cycle, on the effects of the CaL process parameters on the cement kiln energy balance and on the retrofitability of existing cement kilns, the reader is addressed to (De Lena et al., 2017).

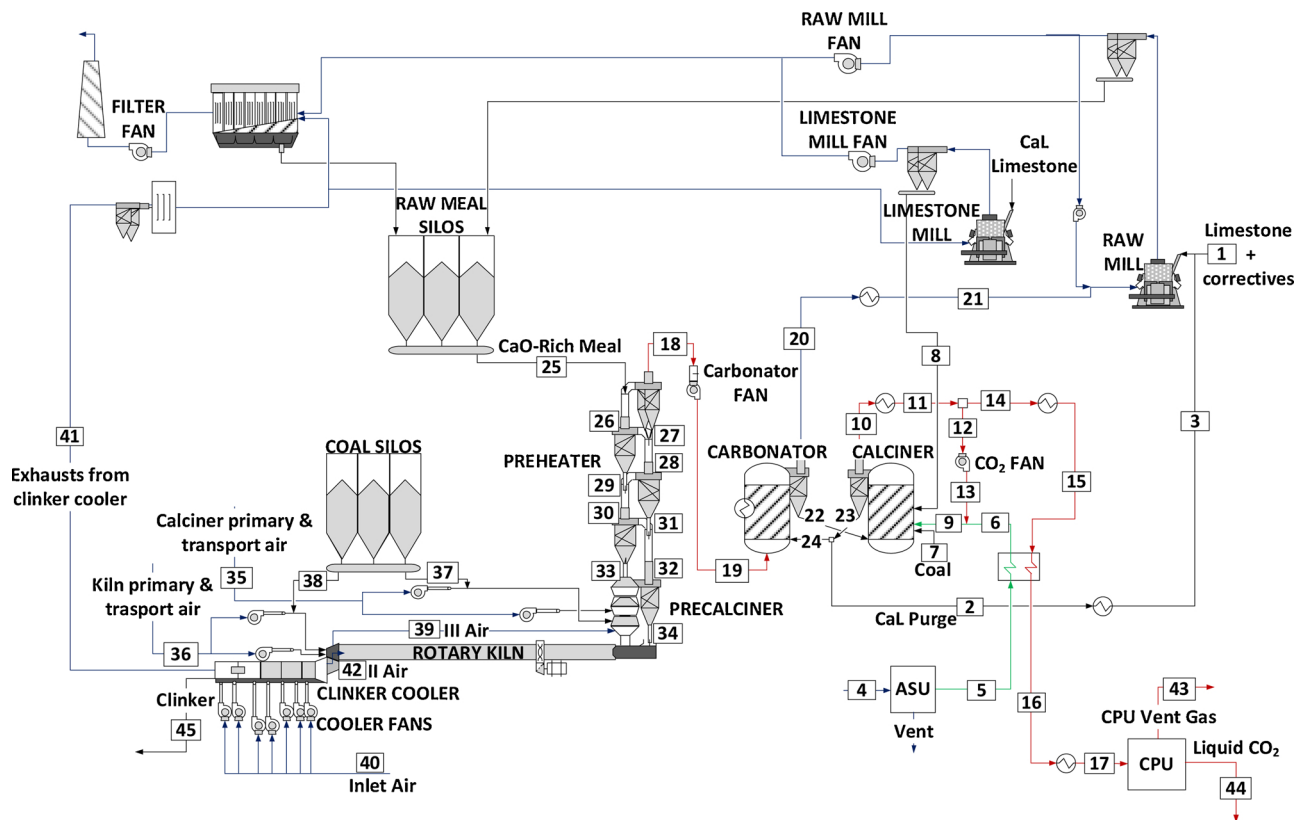


Fig. 1. Schematic of the cement kiln with tail-end CaL process.

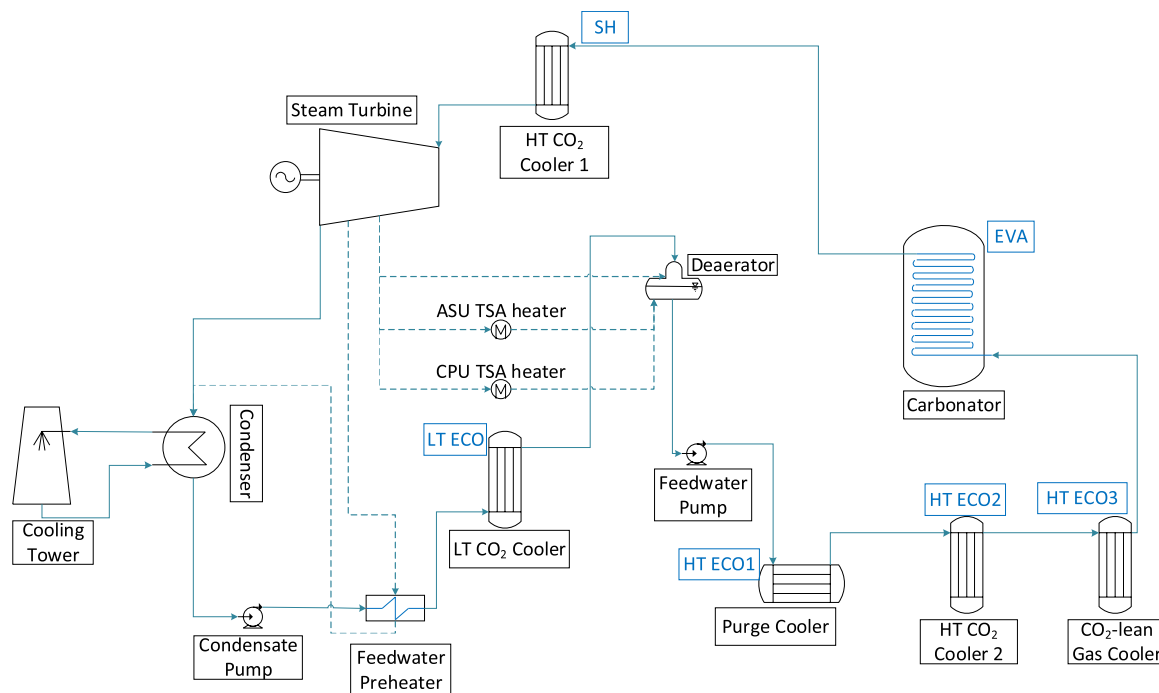


Fig. 2. Schematic of the steam cycle for heat recovery from the tail-end CaL cement kiln.

2.2. Integrated Calcium looping

The flowsheet of the integrated CaL process cement kiln is shown in Fig. 3. This process configuration exploits the cement kiln raw meal as CO₂ sorbent in the CaL process. A single oxyfuel calciner is adopted, representing both the cement kiln precalciner and the CaL calciner. Therefore, this configuration has an intrinsic IL of 100%.

Flue gas from the rotary kiln (stream #5) is cooled in a two-stage raw meal preheater (Fig. 4a). The amount of the raw meal fed to this preheater is tuned to achieve a gas temperature at preheater outlet and carbonator inlet (#6) of 434 °C, which allows achieving the target adiabatic mixing temperature of 600 °C of the solid-gas mixture at the carbonator inlet. The carbonator is a 120 m long gooseneck refractory lined reactor, where about 80% of the inlet CO₂ is captured by the sorbent. Recarbonated solids from the carbonator are partly (30%) sent to the calciner (#7) and partly (65%) sent to a sorbent cooler (#8) to be recirculated to the carbonator itself, whereas the residual amount (5%) escapes the cyclone and is entrained with the decarbonated gas (#9). The internal sorbent recirculation (#8) increases the residence time of

the particles in the carbonator and the average sorbent conversion, allowing to reduce the flow rate of sorbent sent to the calciner (#7) and the fuel consumption for a given target carbon capture efficiency (Spinelli et al., 2018). The oxyfuel calciner is fired with coal (#21) and a 30%vol. O₂ stream, obtained by mixing 95% pure O₂ from the ASU (#19) and a fraction of the calciner off-gas (#25), which is cooled at a temperature of 400 °C and then recycled to the calciner inlet. Combustion provides the heat required for heating and calcining both the recarbonated sorbent (#7) and the preheated raw meal, which comes partly from the two-stage preheater (#4) and partly from a three-stage preheater (#3) using CO₂-rich calciner off-gas at 920 °C (#22) as heat source (Fig. 4b). A fraction of the calcined raw meal (42%) is sent to the rotary kiln (#32), partly (53%) sent to the carbonator after cooling in the sorbent cooler (#30) and partly (5%) entrained with the CO₂-rich gas from the calciner. Carbonator inlet temperature has been demonstrated to be an important parameter for the CO₂ capture efficiency in an adiabatic reactor (Spinelli et al., 2018). For this reason, before being introduced into the carbonator, the hot sorbent (#30) is cooled to 620 °C (#31) in a sorbent cooler (Fig. 4c), by direct contact with

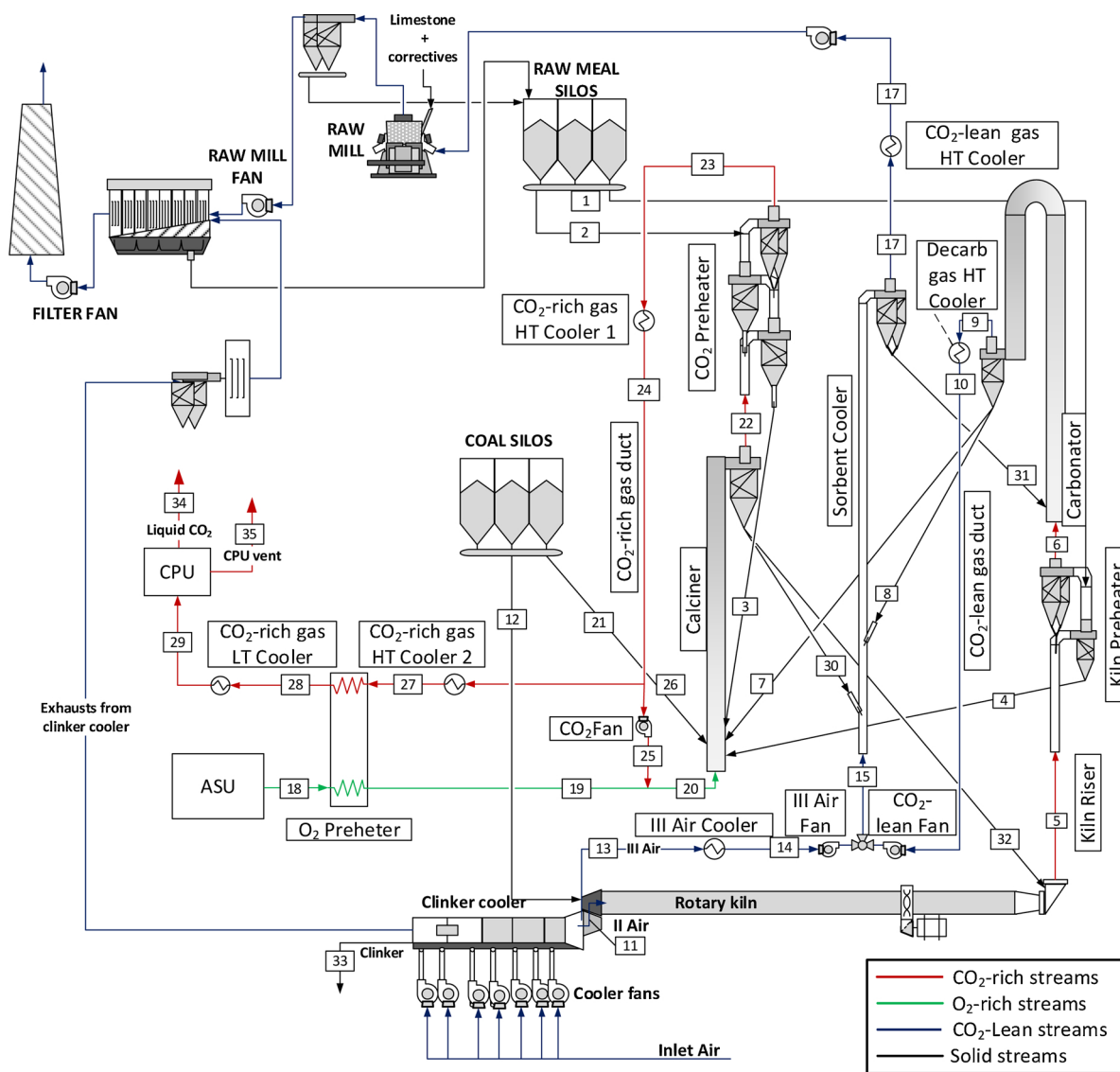


Fig. 3. Schematic of the cement kiln with integrated CaL process.

tertiary air (#14) and carbonator exhaust gas (#10), cooled to 214 °C. Sorbent circulation between the calciner and the carbonator is tuned to achieve a CO₂ capture efficiency in the carbonator of about 80%.

One of the technical uncertainties of the integrated CaL process is related to the high solid-to-gas ratio needed in the carbonator to achieve high CO₂ capture efficiency (Spinelli et al., 2018). In the assessed integrated CaL plant, the resulting solids to gas ratio at the carbonator inlet (including the entrained dust from the last cyclone of the kiln gas preheater) is 13.5 kg/Nm³, to be compared with the 1–1.5 kg/Nm³ in the preheaters of conventional cement kilns. Also in the sorbent cooler, a relatively high solids to gas ratio of 5.1 kg/Nm³ has been obtained compared to conventional cement kiln risers.

Although correlations show that with a gas velocity of 15 m/s no choking should occur in the carbonator with such solids loading (Spinelli et al., 2018), experimental validation of the flow stability in industrially relevant conditions is needed.

Also in the integrated CaL plant, a heat recovery steam cycle must be used to recover the large amount of heat generated in the process (Fig. 5). Steam cycle is based on a superheated Rankine cycle without reheat, with evaporation pressure of 65 bar and SH steam temperature of 460 °C, defined on the basis of conventional steam power plants with similar size (Consonni and Viganò, 2012). High temperature heat is recovered from: (i) tertiary air (III Air coolers) by water preheating, steam evaporation and superheating, (ii) CO₂-lean gas at carbonator

outlet (Decarbonated gas cooler) by high temperature water preheating, (iii) CO₂-lean gas at sorbent cooler outlet (CO₂-lean gas HT cooler) by steam evaporation and (iv) CO₂-rich gas cooler by steam evaporation and water preheating (CO₂-rich gas coolers).

The temperature-heat diagram of the steam cycle of the integrated CaL cement kiln is shown in Fig. 6.

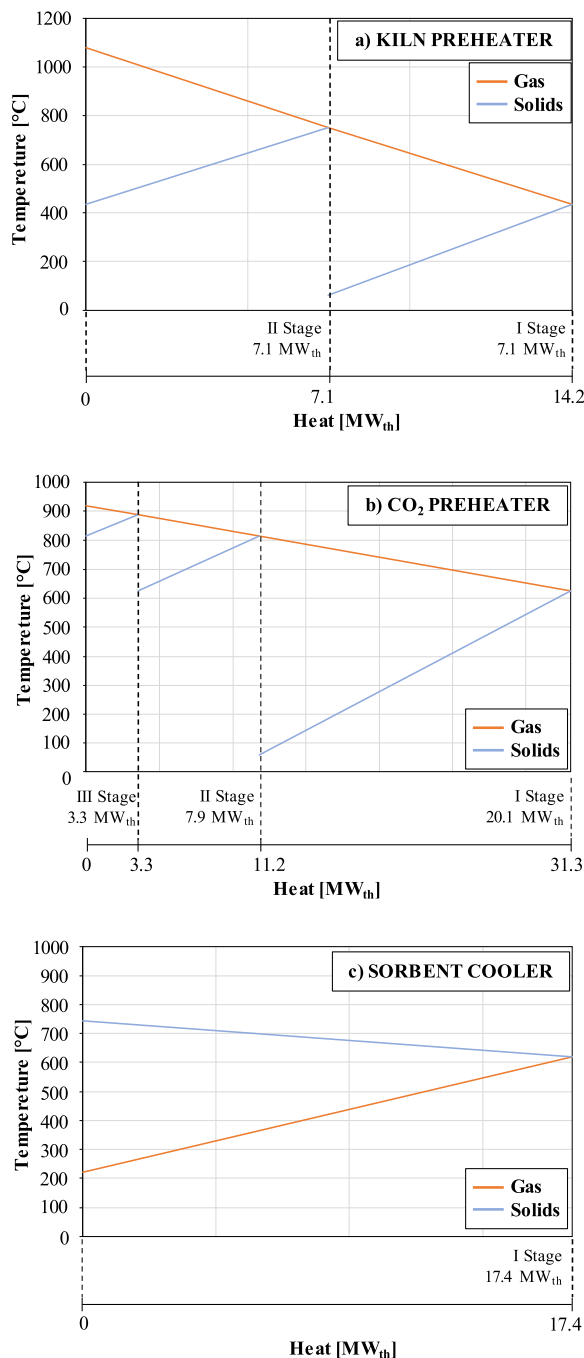


Fig. 4. Temperature-heat diagrams of the preheaters and of the sorbent cooler.

3. Heat and mass balances

3.1. Method

Heat and mass balances are calculated with the in-house process simulation code (GECOS, 2016), which was formerly validated for the calculation of the heat and mass balances of the benchmark cement kiln without CO₂ capture (Campanari et al., 2016). Aspen Plus (AspenTech, 2016) has been used for the calculation of the steam cycle and of the CPU. For the CPU, a model developed by Sintef researchers in the framework of the Cemcap project has been used (Jamali et al., 2018), allowing a consistent comparison between the CaL and the oxyfuel cement kiln technologies. Fluidized bed and entrained flow carbonators have been simulated with the Matlab models described in (Romano, 2012) and (Spinelli et al., 2018) respectively.

For a detailed discussion of the calculation methodology and assumptions of the cement plant with the tail-end CaL system, the reader is addressed to (De Lena et al., 2017). In the present work, cases with integration level of 20% and 50% presented in (De Lena et al., 2017) have been selected as representative cases of the technology. It must be noted that the performance indicators of the tail-end plants in this work slightly differ from the previous study by the same authors (De Lena et al., 2017), because of the new model used for the calculation of the CPU and because of additional consumptions of auxiliaries for heat rejection by cooling tower.

Simulation assumptions for the calculation of the integrated CaL cement kiln are consistent with the CEMCAP project framework (Anantharaman et al., 2017). Differently from limestone, where an abundant literature on its properties as CO₂ sorbent is available, the capacity of raw meal as CO₂ sorbent cannot be satisfactorily predicted from the number of carbonation-calcination cycles only, as it strongly depends on the level of aggregation between Ca and SiO₂ and on the calcination conditions (Alonso et al., 2017; Arias et al., 2017b). Due to the lack of experimental data on the CaL process in industrially relevant conditions, it is not possible to define a reliable correlation for the sorbent capacity and a maximum CaO to CaCO₃ conversion degree after the fast kinetically controlled period (X_{max}) of 0.40 has been assumed. The sorbent circulation rate between the calciner and the carbonator has been assumed equal to 3.32 kg/Nm³ (corresponding to F_{Ca}/F_{CO_2} of 3.9). Sorbent recirculation in the carbonator of 65% has been assumed. According to the carbonator model, the combination of the assumed sorbent circulation and sorbent recirculation leads to a carbonator outlet temperature of about 670 °C and a CO₂ capture efficiency of 82%.

For the heat recovery steam cycle, steam parameters and steam turbine efficiency has been assumed according to (Consonni and Viganò, 2012) and are representative of the current technology for steam turbines with gross power output of 20–30 MW_e. Steam parameters and turbine efficiency in the integrated CaL case are lower than in the tail-end case (evaporation pressure 65 bar vs. 100 bar, SH temperature 460 °C vs. 530 °C, turbine isentropic efficiency 78.9% vs. 85.7%), due to the smaller size of the steam cycle.

The main assumptions used for the calculation of the mass and energy balances of the integrated CaL plant are resumed in Table 1.

Energy and environmental performance are evaluated through the key performance indicators defined in equations (2)(4). Equivalent fuel consumption q_{eq} is computed with Eq. (2) as the sum of the direct fuel consumption of the cement kiln (q) and the indirect fuel consumption associated to the electricity imported by the plant from the electric grid

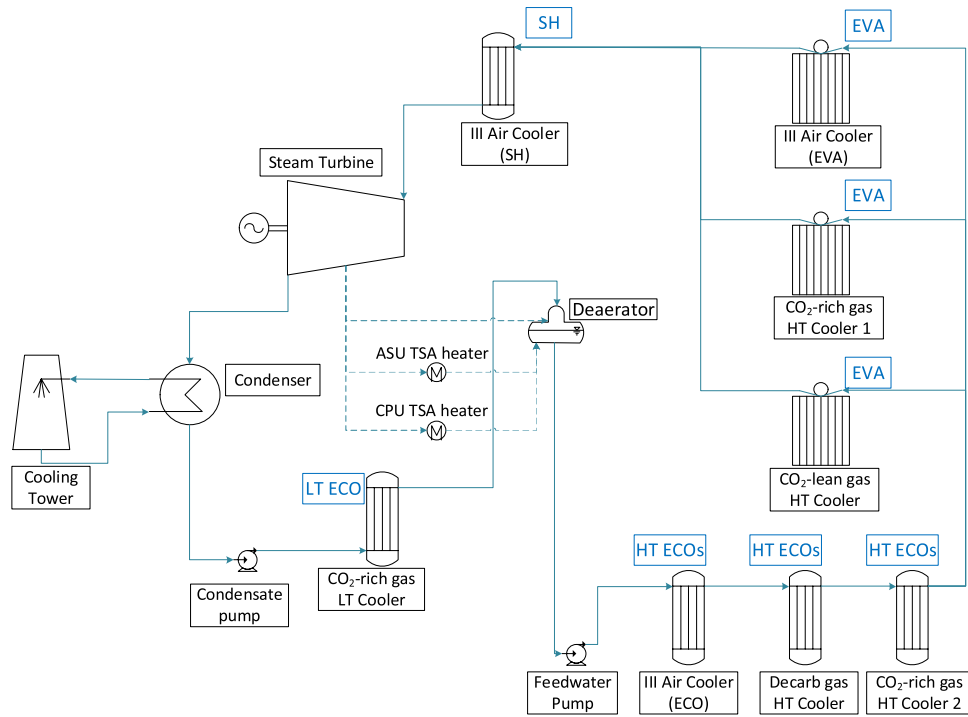


Fig. 5. Schematic of the steam cycle for heat recovery from the integrated CaL cement kiln.

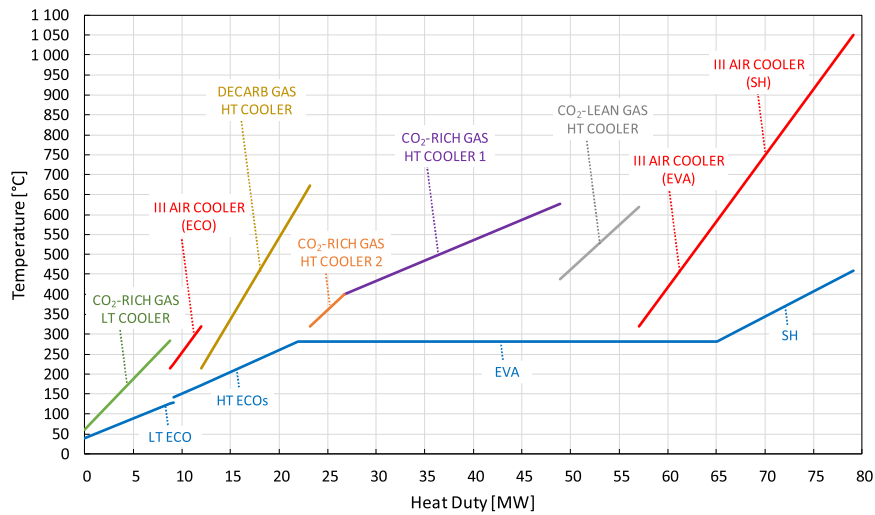


Fig. 6. Temperature-heat diagram of the steam cycle of the integrated CaL plant, shown in Fig. 5.

(P_e/η_e) . Equivalent CO_2 emissions $e_{CO_2,eq}$ are computed with Eq. (3) as the sum between the direct emissions from the cement kiln (e_{CO_2}) and the indirect emissions associated to the electricity imported from the electric grid ($P_e \cdot E_{CO_2,e}$), which depend on the specific CO_2 emissions associated to power generation ($E_{CO_2,e}$). It must be noted that in the tail-end CaL plants with sufficiently low IL, the steam cycle generates electricity in excess compared to the auxiliaries. In this case, the cement plant becomes a net electricity producer ($P_e < 0$), leading to negative indirect fuel consumptions and emissions (i.e. fuel and emissions

credits). The specific primary energy consumption for CO_2 avoided ($SPECCA$) is then calculated with Eq. (4), with respect to the reference cement kiln without CO_2 capture (ref).

$$q_{eq} = q + \frac{P_e}{\eta_e} \quad (2)$$

$$e_{CO_2,eq} = e_{CO_2} + P_e \cdot E_{CO_2,e} \quad (3)$$

Table 1
Main assumptions for the simulation of the cement kiln with integrated CaL.

| <i>Clinker burning process</i> | |
|--|--------|
| Clinker production [tpd] | 2817 |
| Clinker/cement factor [kg _{clik} /kg _{cem}] | 0.737 |
| Electric consumption of auxiliaries [kWh _e /t _{cem}] | 97 |
| Primary and transport air to rotary kiln [Nm ³ /kg _{coal}] | 1.74 |
| Secondary air to rotary kiln [Nm ³ /t _{clik}] | 272.3 |
| Rotary kiln gas outlet temperature [°C] | 1078.4 |
| Secondary air temperature [°C] | 1137 |
| Tertiary air temperature [°C] | 1049.8 |
| Clinker temperature at cooler outlet [°C] | 114.9 |
| Temperature of solids after milling [°C] | 60 |
| Preheaters cyclones efficiency [%] | 86 |
| Heat losses from rotary kiln [kJ _{th} /kg _{clik}] | 180.2 |
| Heat losses from clinker cooler [kJ _{th} /kg _{clik}] | 11.13 |
| Air in-leakages into rotary kiln [Nm ³ /t _{clik}] | 12.01 |
| <i>Ca-Looping process</i> | |
| Maximum CaO to CaCO ₃ conversion degree (X _{max}) [-] | 0.40 |
| Sorbent recirculation in the carbonator [%] | 66 |
| Sorbent circulation rate from calciner to carbonator [kg/Nm ³] | 3.32 |
| Gas superficial velocity at carbonator inlet [m/s] | 15 |
| Adiabatic gas/solid mixing temperature at carbonator inlet [°C] | 600 |
| Calciner outlet temperature [°C] | 920 |
| Raw meal calcination degree at calciner outlet [%] | 89.1 |
| Pressure losses in calciner and CO ₂ Tower [kPa] | 11 |
| Pressure losses in sorbent cooler [kPa] | 4 |
| Pressure losses in carbonator [kPa] | 4 |
| Recirculated CO ₂ -rich gas temperature [°C] | 400 |
| Oxygen preheating temperature [°C] | 150 |
| Cyclones efficiency [%] | 95 |
| Oxygen concentration in oxidant flow to calciner [%vol.] | 30 |
| Oxygen concentration in calciner off-gas [%vol.] | 5 |
| Fans isentropic efficiency [%] | 82 |
| Fans electric-mechanical efficiency [%] | 94 |
| Auxiliaries for calciner fuel grinding [kWh _e /t _{coal}] | 14 |
| <i>Air separation unit</i> | |
| Oxygen purity [%vol.] | 95 |
| Electric consumption [kWh _e /tO ₂] | 230 |
| LP steam consumption for TSA regeneration [kJ _{th} /kgO ₂] | 58.3 |
| <i>Heat recovery steam cycle</i> | |
| Evaporation pressure [bar] | 65.2 |
| Superheated steam temperature [°C] | 460 |
| Condensation pressure [bar] | 0.07 |
| Steam turbine isentropic efficiency [%] | 78.9 |
| Gearbox and electric generator mechanical-electric efficiency [%] | 94 |
| Feedwater pump hydraulic efficiency [%] | 75 |
| Feedwater pump mechanical-electric efficiency [%] | 94 |
| Electric consumption for heat rejection to ambient [% of the heat rejected] | 1 |
| Pressure drop in the economizer [bar] | 20 |
| Pressure drop in the superheater [%] | 8 |
| Pressure drop in the turbine admission valve [%] | 5 |
| Deaerator temperature [°C] | 140 |
| Pressure drop of the steam to the deaerator [%] | 7 |
| Pinch point temperature difference [°C] | 20 |
| <i>CO₂ compression and purification unit</i> | |
| Pressure in the liquid-vapor separator [bar] | 20-23 |
| Temperature in the liquid-vapor separator [°C] | -50 |
| Number of LP/HP intercooled compression stages | 4 / 2 |
| Minimum ΔT in the main heat exchanger [°C] | 3 |
| Temperature at intercoolers outlet [°C] | 28 |
| Compressors isentropic efficiency LP/HP [%] | 85 |
| Compressors mechanical efficiency LP/HP [%] | 95 |
| Last stage compressor discharge pressure [bar] | 84 |
| Pump hydraulic efficiency [%] | 80 |
| Pump mechanical efficiency [%] | 95 |
| CO ₂ target purity [%vol.] | > 95% |
| CO ₂ delivery pressure [bar] | 110 |
| CO ₂ delivery temperature [°C] | 37 |
| Equivalent electric consumption for dehydration [MJ _{th} /kgH ₂ O] | 16.6 |

$$SPECCA = \frac{q_{eq} - q_{eq,ref}}{e_{CO_2,eq,ref} - e_{CO_2,eq}} \quad (4)$$

For the calculation of the indirect fuel consumption and emissions, a reference power generation scenario must be defined with the related electric efficiency η_e and carbon intensity $E_{CO_2,e}$. In this work, out of the several possible scenarios defined in the CEMCAP project (Anantharaman et al., 2017) two scenarios have been considered: (i) the average EU-28 non-CHP energy mix of year 2015 ($\eta_e = 45.9\%$, $E_{CO_2,e} = 262 \text{ kg}_{CO_2}/\text{MWh}_e$) and (ii) a pulverized coal USC power plant ($\eta_e = 44.2\%$, $E_{CO_2,e} = 770 \text{ kg}_{CO_2}/\text{MWh}_e$). This second case has been selected among the different proposed scenarios, as it represents the state-of-the-art power generation technology using the same fuel of the cement kiln.

3.2. Results

The main results of the mass and energy balances are reported in Table 2. The properties of the streams of the plant are reported in the appendix in Table A1.

All the CaL cases involve an increased fuel consumption compared to the reference cement kiln without CO₂ capture. The integrated CaL case has the lowest increase (+67%), followed by the tail-end 50%-IL case (+119%) and the tail-end 20%-IL case (+170%). The lower fuel consumption of the integrated CaL case is substantially due to the fact that only the CO₂ generated in the rotary kiln is captured in the CaL carbonator and requires heat for sorbent regeneration. Conversely, in the tail-end cases, the fluidized bed carbonator is fed with all the CO₂-rich off-gas released by the cement kiln preheater, including CO₂ released by CaCO₃ calcination in the air-fired calciner. Hence, the CO₂ generated by raw meal decomposition experiences a double calcination process, the first one in the air-blown precalciner and the second one in the oxyfuel CaL calciner for regenerating the carbonated sorbent. This double calcination process is responsible for the higher fuel consumption calculated for the tail-end plants compared to the integrated ones. For the same reason, tail-end cases with lower IL need higher fuel input, since a higher portion of the inlet CaCO₃ is calcined in the cement kiln air-blown precalciner, leading to double calcination of the associated CO₂, rather than in the oxyfuel CaL calciner, requiring a single oxy-fuel calcination step.

In all the cases assessed, there are minor changes in the fuel input to the rotary kiln (the highest being a 7% reduction in the integrated CaL case, resulting from the higher temperature of the inlet calcined raw meal produced in the oxyfuel precalciner). In the tail-end cases, about 70% of the total fuel input is burned in the CaL calciner, whereas the residual fraction is burned in the cement burning line (i.e. in the rotary kiln and in the precalciner). Fuel consumption in the cement kiln is between 14 and 36% less than in the reference kiln, thanks to the reduced fuel demand in the precalciner, which is partly fed with the preheated CaO-rich material purged from the CaL unit. In the integrated CaL case, the CaL calciner coincides with the precalciner and consumes 79% of the total fuel input. The fuel balance of the different systems is graphically shown in Fig. 7a.

The total CO₂ capture efficiency, computed as the ratio between the CO₂ to storage and the total CO₂ generated by fuel combustion and raw meal calcination, is higher in the integrated CaL case (94.6% vs. 91.4–93.6% of the two tail-end cases) despite the lower CO₂ capture efficiency of the carbonator (82.0% vs. 88.8–90.0%) because of two reasons. The first one is that the carbonator of the integrated CaL plant treats only the rotary kiln off-gas, while all the CO₂ generated in the oxyfuel calciner is captured with nearly 100% efficiency, typical of the

Table 2
Main results from the mass and energy balances of CaL cement kilns and of the benchmark cement kiln without CO₂ capture.

| | Cement kiln w/o CCS | | Tail-end 20%-IL CaL | | Tail-end 50%-IL CaL | | Integrated CaL | |
|--|---------------------|--------|---------------------|--------|---------------------|--------|----------------|--------|
| IL, % | – | – | 20 | – | 50 | – | – | – |
| F_0/F_{CO_2} | – | – | 0.16 | – | 0.60 | – | 3.96 | – |
| F_{CaL}/F_{CO_2} | – | – | 4.78 | – | 2.94 | – | 3.90 | – |
| Direct fuel consumption (q), MW _{LHV} – MJ _{LHV} /kg _{clik} | 105.9 | 3.24 | 285.9 | 8.72 | 232.2 | 7.10 | 177.2 | 5.44 |
| Fuel consumption in the rotary kiln, MW _{LHV} – MJ _{LHV} /kg _{clik} | 40.2 | 1.23 | 39.9 | 1.22 | 39.9 | 1.22 | 37.5 | 1.15 |
| Fuel consumption in the precalciner, MW _{LHV} – MJ _{LHV} /kg _{clik} | 65.7 | 2.01 | 50.8 | 1.55 | 27.6 | 0.85 | – | – |
| Fuel consumption in the CaL calciner, MW _{LHV} – MJ _{LHV} /kg _{clik} | – | – | 195.2 | 5.95 | 164.6 | 5.04 | 139.8 | 4.29 |
| Oxygen Input, t/day – kg _{O2} /kg _{clik} | – | – | 1453.9 | 0.51 | 1236.2 | 0.44 | 1057.6 | 0.38 |
| CO ₂ capture efficiency of the carbonator, % | – | – | 88.8% | – | 90.0% | – | 82.0% | – |
| CO ₂ generated from fuel combustion, kg/s – kg _{CO2} /t _{clik} | 9.87 | 301.8 | 26.64 | 812.6 | 21.63 | 661.6 | 16.52 | 506.6 |
| CO ₂ generated from raw meal calcination, kg/s – kg _{CO2} /t _{clik} | 18.42 | 563.4 | 18.44 | 562.4 | 18.73 | 572.9 | 17.85 | 547.5 |
| Captured CO ₂ to storage, kg/s – kg _{CO2} /t _{clik} | – | – | 41.20 | 1256.6 | 37.78 | 1155.5 | 32.51 | 997.1 |
| Total CO ₂ capture efficiency, % | – | – | 91.4% | – | 93.6% | – | 94.6% | – |
| Direct CO ₂ emission from kiln flue gas, kg/s – kg _{CO2} /t _{clik} | 28.3 | 865.2 | 2.6 | 79.5 | 1.6 | 48.0 | 0.8 | 25.7 |
| Direct CO ₂ emission from the CPU, kg/s – kg _{CO2} /t _{clik} | – | – | 1.3 | 39.0 | 1.0 | 31.1 | 1.0 | 31.3 |
| Total direct CO ₂ emission (e _{CO2}), kg/s – kg _{CO2} /t _{clik} | 28.3 | 865.2 | 3.9 | 118.5 | 2.6 | 79.1 | 1.9 | 57.0 |
| Direct emission reduction, % | – | – | 86.3% | – | 90.9% | – | 93.4% | – |
| Power balance | | | | | | | | |
| Gross steam turbine electricity production, MW _e – kWh _e /t _{clik} | – | – | 66.16 | 560.6 | 41.58 | 353.2 | 21.90 | 186.6 |
| Steam cycle pumps, MW _e – kWh _e /t _{clik} | – | – | –1.28 | –10.9 | –0.80 | –6.8 | –0.34 | –2.9 |
| Auxiliaries for steam cycle heat rejection, MW _e – kWh _e /t _{clik} | – | – | –1.11 | –9.4 | –0.78 | –6.6 | –0.49 | –4.2 |
| ASU consumption, MW _e – kWh _e /t _{clik} | – | – | –13.69 | –116.0 | –11.64 | –98.9 | –9.96 | –84.9 |
| Fans in CaL system, MW _e – kWh _e /t _{clik} | – | – | –2.97 | –25.2 | –2.70 | –22.9 | –1.21 | –10.3 |
| CO ₂ compression, MW _e – kWh _e /t _{clik} | – | – | –17.60 | –149.0 | –16.11 | –136.9 | –14.11 | –120.2 |
| Power consumption for cooling system, MW _e – kWh _e /t _{clik} | – | – | –0.74 | –6.3 | –0.67 | –5.7 | –0.58 | –5.0 |
| Auxiliaries for calciner fuel grinding, MW _e – kWh _e /t _{clik} | – | – | –0.22 | –1.8 | –0.18 | –1.5 | –0.26 | –2.2 |
| Cement plant auxiliaries, MW _e – kWh _e /t _{clik} | –15.49 | –131.6 | –15.53 | –131.6 | –15.49 | –131.6 | –15.36 | –130.9 |
| Net electricity production, MW _e – kWh _e /t _{clik} | –15.49 | –131.6 | 13.01 | 110.3 | –6.79 | –57.7 | –20.41 | –173.9 |
| Net electricity production, kWh _e /t _{tem} | –97.0 | – | 81.3 | – | –42.5 | – | –128.2 | – |

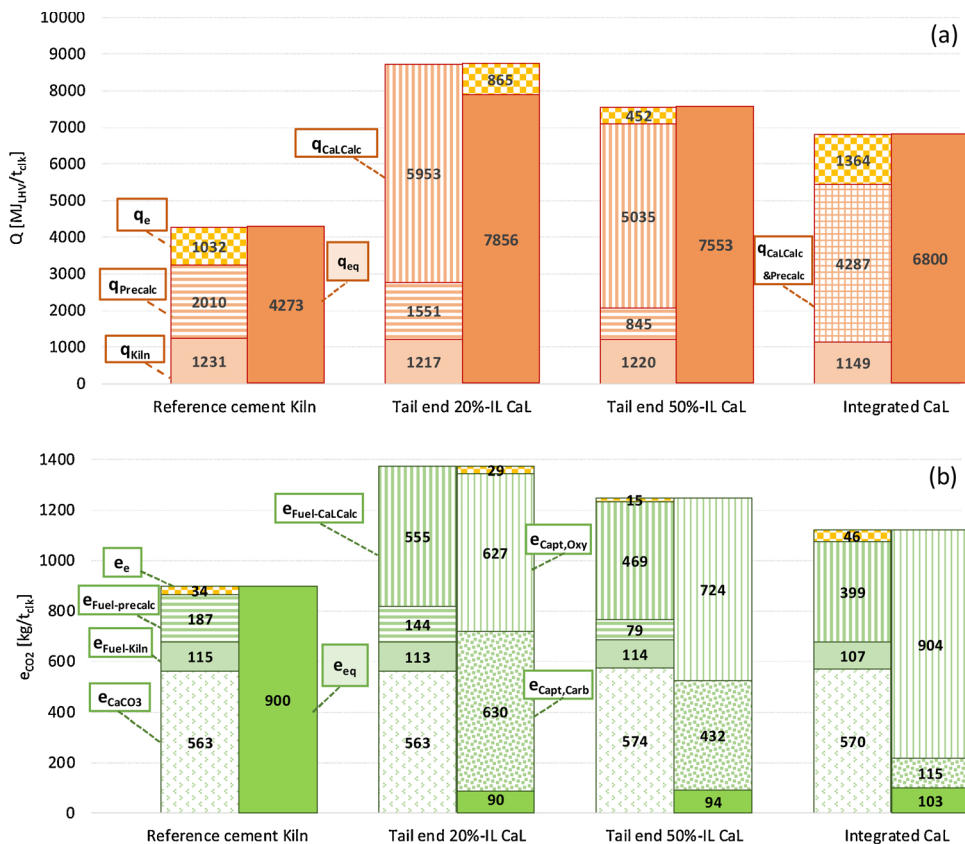


Fig. 7. (a) Fuel balance. Left column: fuel consumed in the different combustion zones and indirect fuel consumption; right column: equivalent fuel consumption and indirect fuel saving. (b) CO₂ balance. Left column: CO₂ generation sources, including indirect CO₂ emissions; right column: CO₂ captured, emitted and indirect CO₂ avoided. e_{Capt,Oxy} indicates the CO₂ captured by oxyfuel combustion (i.e. CO₂ generated from fuel burned in oxyfuel conditions + CO₂ generated from first calcination of CaCO₃ in the oxyfuel calciner). e_{Capt,Carb} indicates the CO₂ captured by reaction with CaO sorbent in the carbonator.

Table 3Key performance indicators of the CaL cement kilns and the benchmark cement kiln without CO₂ capture under different electricity production scenarios.

| | Cement kiln w/o CCS | | Tail-end 20%-IL CaL | | Tail-end 50%-IL CaL | | Integrated CaL | |
|---|---------------------|-------|---------------------|--------|---------------------|-------|----------------|-------|
| Direct fuel consumption (q), MW _{LHV} – MJ _{LHV} /kg _{clik} | 105.9 | 3.24 | 285.9 | 8.72 | 232.2 | 7.10 | 177.2 | 5.44 |
| Direct CO ₂ emission (e_{CO_2}), kg/s – kg _{CO2} /t _{clik} | 28.3 | 865.2 | 3.9 | 118.5 | 2.6 | 79.1 | 1.9 | 57.0 |
| Net electricity consumption (P_e), MW _e – kWh _e /t _{clik} | 15.49 | 131.6 | –13.01 | –110.3 | 6.79 | 57.7 | 20.41 | 174.0 |
| <i>State of the art pulverized coal USC power plant ($\eta_e = 44.20\%$, $E_{CO_2,e} = 770$ kg_{CO2}/MWh_e)</i> | | | | | | | | |
| Indirect fuel consumption (q_e), MW _{LHV} – MJ _{LHV} /kg _{clik} | 35.0 | 1.07 | –29.4 | –0.90 | 15.4 | 0.47 | 46.2 | 1.42 |
| Equivalent fuel consumption (q_{eq}), MW _{LHV} – MJ _{LHV} /kg _{clik} | 141.0 | 4.31 | 256.5 | 7.82 | 247.5 | 7.57 | 223.4 | 6.85 |
| Indirect CO ₂ emission ($e_{CO_2,e}$), kg/s – kg _{CO2} /t _{clik} | 3.3 | 101.3 | –2.8 | –84.9 | 1.5 | 44.4 | 4.4 | 133.9 |
| Equivalent CO ₂ emission ($e_{CO_2,eq}$), kg/s – kg _{CO2} /t _{clik} | 31.6 | 966.6 | 1.1 | 33.6 | 4.0 | 123.5 | 6.2 | 190.9 |
| Equivalent fuel consumption increase, % | – | – | 81.4% | – | 75.5% | – | 58.9% | – |
| Equivalent emission reduction, % | – | – | –96.5% | – | –87.2% | – | –80.3% | – |
| SPECCA, MJ _{LHV} /kg _{CO2} | – | – | 3.76 | – | 3.86 | – | 3.27 | – |
| <i>EU-28 non-CHP energy mix (2015) ($\eta_e = 45.9\%$, $E_{CO_2,e} = 262$ kg_{CO2}/MWh_e)</i> | | | | | | | | |
| Indirect fuel consumption (q_e), MW _{LHV} – MJ _{LHV} /kg _{clik} | 33.7 | 1.03 | –28.4 | –0.86 | 14.8 | 0.45 | 44.5 | 1.36 |
| Equivalent fuel consumption (q_{eq}), MW _{LHV} – MJ _{LHV} /kg _{clik} | 139.7 | 4.27 | 257.6 | 7.86 | 247.0 | 7.55 | 221.7 | 6.80 |
| Indirect CO ₂ emission ($e_{CO_2,e}$), kg/s – kg _{CO2} /t _{clik} | 1.1 | 34.5 | –0.9 | –28.9 | 0.5 | 15.1 | 1.5 | 45.6 |
| Equivalent CO ₂ emission ($e_{CO_2,eq}$), kg/s – kg _{CO2} /t _{clik} | 29.4 | 899.7 | 2.9 | 89.6 | 3.1 | 94.2 | 3.3 | 102.5 |
| Equivalent fuel consumption increase, % | – | – | 83.8% | – | 76.7% | – | 59.1% | – |
| Equivalent emission reduction, % | – | – | –90.0% | – | –89.5% | – | –88.6% | – |
| SPECCA, MJ _{LHV} /kg _{CO2} | – | – | 4.42 | – | 4.07 | – | 3.17 | – |

oxyfuel process. On the contrary, the carbonator of the tail-end cases treats the entire CO₂ flow rate generated in the rotary kiln and in the air-blown calciner, resulting in a higher CO₂ slip compared to the total CO₂ generated in the plant despite the higher carbonator efficiency. The second reason is related to the higher fuel consumption of the tail-end cases, which determines the generation of a higher CO₂ flow rate in the CaL calciner and therefore a higher CO₂ loss from the CO₂ purification unit. Therefore, also the direct CO₂ emission reduction is lower in the tail-end cases (86.3–90.9%) compared to the integrated CaL case (93.4%). For better clarity, the CO₂ balance of the different systems is graphically reproduced in Fig. 7b.

As for the power plant, a general result obtained is that the higher the total fuel consumption in the CaL system, the higher the thermal power recovered by the steam cycle. Therefore, the tail-end CaL 20%-IL plant is the plant configuration with the highest steam turbine power (66.2 MW_e), which overcomes the electric consumption related to the CO₂ capture section (mainly associated to CO₂ compression and O₂ production) and to the other conventional cement plant auxiliaries (14.27 MW_e, or 89.1 kWh_e/t_{cem}). Therefore, the cement kiln integrated with this tail-end CaL configuration (20%-IL) becomes a co-producer of cement and electricity, with a net power output of 13 MW_e. In the tail-end CaL 50%-IL plant, the steam turbine generates a lower gross power (41.58 MW_e), which is high enough to compensate the CO₂ capture island auxiliaries and part of the conventional cement plant parasitic consumptions, but not enough to export electricity to the grid. As a result, the plant remains a net importer of electricity, although power absorption is 56% less than in the reference cement plant without CO₂ capture (42.5 vs. 97 kWh_e/t_{cem}). In the integrated CaL case, steam turbine power is 21.98 MW_e, which mostly compensates the power absorption of the CO₂ capture island. Net electricity consumption in this case is 20.4 MW_e or 128 kWh_e/t_{cem}, corresponding to an increase of 32% with respect to the power absorbed by the reference cement plant without CO₂ capture.

In Table 3, the key performance indicators of the assessed plants are reported for the two power generation scenarios considered in this work and introduced in Section 3.1. Negative indirect fuel consumption and CO₂ emissions are obtained in the tail-end 20%-IL case, thanks to the net power export. Therefore, equivalent fuel consumption and emissions are lower than the direct ones. On the contrary, equivalent fuel consumption and emissions of the other CaL cases are higher than the direct consumptions and emissions because of the net electricity import. As a result, equivalent emissions reduction becomes higher in the tail-end 20%-IL CaL case compared to the other cases. The effect is amplified in the USC power generation scenario, mainly due to the higher carbon intensity of the electricity exchanged with the grid. On the other hand, the equivalent fuel consumption remains the highest in the tail-end 20%-IL case, despite the effect of power export.

The best SPECCA is obtained for the integrated CaL case, ranging between 3.17 and 3.27 MJ_{LHV}/t_{CO2}, depending on the power generation scenario assumed for the electric grid. For the tail-end CaL plants, SPECCA of 3.86–4.07 MJ_{LHV}/t_{CO2} and 3.76–4.42 MJ_{LHV}/t_{CO2} have been calculated for the 50%-IL and 20%-IL cases respectively.

As outlined in Table 3, most key performance indicators (indirect CO₂ emissions, total CO₂ emission reduction, indirect fuel consumption and SPECCA) change depending on the parameters (i.e. carbon intensity and fuel-to-electricity conversion efficiency) of the power generation scenario considered. More specifically, the lower the carbon intensity of the electric mix, the lower the indirect CO₂ emissions due to electricity imports. This is a positive contribution for the integrated and the tail-end 50%-IL cases, which are net power importer, whereas for the tail-end 20%-IL case, this contribution is negative since it represents indirect CO₂ emissions savings, due to the surplus of electricity exported. It is worth highlighting that, in case a more aggressive GHG reduction scenario is considered, e.g. the beyond 2 °C scenario of IEA (IEA, 2017) for which the CO₂ intensity of global electricity generation is expected to fall below zero by 2060 (–10 g_{CO2}/kWh), the cases

without electric export will be even more advantageous than the 20%-IL scheme, from the point of view of both total emissions reduction and SPECCA, as a result of the reduction of the indirect CO₂ emissions.

4. Economic analysis

4.1. Method

The method for the economic analysis performed in this work has been defined in the framework of the CEMCAP project (Anantharaman et al., 2017; Voldsund et al., 2018). An Excel spreadsheet has been developed for the calculation of the cost of cement (COC) and the cost of CO₂ avoided (CCA) according to the CEMCAP method (De Lena et al., 2018).

The main financial assumptions are reported in Table 4.

Assumptions for the calculation of Capex and Opex are reported in Table 5.

Total plant cost (TPC) of each item is estimated with Eq. (5), by increasing the total direct costs (TDC) by the indirect cost factor (INCF), the owner's cost factor (OCF) and the project contingencies factor (CF_{project}). Total direct costs are estimated with eq.(6), as the sum of the equipment cost (EC), the installation cost (IC), increased by process contingency factor (CF_{process}).

$$TPC = TDC \cdot (1 + INCF + OCF + CF_{project}) \quad (5)$$

$$TDC = (EC + IC) \cdot (1 + CF_{process}) \quad (6)$$

To estimate the equipment cost (EC), functions reported in Table 6 have been used, most of which taken or adapted from (Cinti et al., 2018).

As indicated in Table 6, two different process contingency factors have been assumed for the different items (Voldsund et al., 2018), expressed as percentage of the installed equipment cost. The first process contingency factor depends on the maturity of the technology, i.e. on its technology readiness level (TRL). For the tail-end CaL reactors, which is considered a TRL6 technology, based on the significant experimental experience with fluidized bed CaL reactors at significant scale and industrially relevant operating conditions (Arias et al., 2013; Hornberger et al., 2017; Kremer et al., 2013), process contingencies have been assumed equal to 20%. For the integrated CaL plant, which is considered at TRL3, process contingencies of 60% have been assumed for the CaL reactors. For the CPU, process contingencies are equal to 20%. For other standard components (preheaters, fans, steam cycle, ASU), process contingency of 5% are assumed. The second process contingency factor depends on the level of detail of the equipment list used to estimate the

Table 4

Assumptions for the economic analysis.

| | |
|--|-------------------|
| Cost basis | € ₂₀₁₄ |
| Capacity factor, % | 91.3 |
| Tax rate, % | 0 |
| Operational life, yrs | 25 |
| Construction time for cement kiln, yrs | 2 |
| Construction time for CO ₂ capture plant, yrs | 3 |
| Percentage of TPC depreciated, % | 100 |
| Inflation rate, % | 0 |
| Discount rate, % | 8 |

Table 5

Assumptions for Capex and Opex calculations.

| CAPEX | |
|---|-------------|
| Process conting. of CO ₂ capture plant (maturity), %(EC + IC) | see Table 6 |
| Process conting. of CO ₂ capture plant (level of detail of equipment list), %(EC + IC) | see Table 6 |
| Indirect costs factor (INCF), %TDC | 14 |
| Owner's costs factor (OCF), %TDC | 7 |
| Project contingencies factor (CF _{project}), %TDC | 15 |
| VARIABLE OPEX | |
| Raw meal price, €/t | 3.012 |
| Coal, €/GJ _{LHV} | 3 |
| Electricity, €/MWh _e | 58.1 |
| Cooling water, €/m ³ | 0.39 |
| Carbon tax, €/t _{CO2} | 0 |
| Ammonia price for SNCR, €/t _{NH3} | 0.13 |
| Other variable O&M costs, €/t _{cem} | 0.8 |
| FIXED OPEX | |
| Insurance and local tax, %TPC/year | 2 |
| Maintenance cost, %TPC/year | 2.5 |
| Number of employees in cement kiln | 100 |
| Number of employees in CO ₂ capture plant | 20 |
| Cost of labor, k€/y per person | 60 |
| Maintenance labor, % of maintenance cost | 40 |
| Administrative and support labor, % O&M labor cost | 30 |

equipment cost. It has been assumed equal to 12% of the installed equipment cost and has been applied only to the CaL reactors and the CPU.

To calculate the Capex of the plants with CO₂ capture, the TPC calculated for the CO₂ capture plant with the method described above is summed to the depreciated cost of the existing cement plant, which is equal to 203.7 M€. This calculation approach, with a value of the existing cement plant independent of the capture plant, reflects the methodology followed for evaluating retrofit projects. It can be observed that the integrated CaL case is penalized by this approach compared to a greenfield project, since the existing equipment of the preheater are assumed to be substituted by the new equipment for the CaL process.

Once Capex and Opex have been defined, the cost of clinker and cement (COC) are calculated as the breakeven selling price leading to a net present value of the project equal to zero. The cost of CO₂ avoided is calculated with Eq. (7), as the ratio between the differential COC and the differential equivalent specific emissions of the cement plant with CO₂ capture and the reference cement plant without capture.

$$CCA = \frac{COC - COC_{ref}}{e_{CO2,eq,ref} - e_{CO2,eq}} \quad (7)$$

4.2. Results

In Table 7, the breakdown of the total plant cost is reported for the CaL plants. In all cases, the largest cost (more than 50% of the cost of the capture plant) is associated to the ASU and the CPU. In the tail-end cases, a significant share of the cost is associated to the fluidized bed

Table 6
Assumptions for the calculation of the capital costs of cement plants with CO₂ capture.

| Item | EC function [M€ ₂₀₁₄] | Installation cost factor [% of EC] | Process contingencies factor (maturity) [% of EC + IC] | Process contingencies factor (details of equipment list item) [% of EC + IC] |
|--|---|---|--|--|
| Existing cement plant | 149.8 | – | – | – |
| Limestone grinding plant | $EC = 1.3 \cdot \left(\frac{m_{RawMeal} [tph]}{30} \right)^{0.67}$ | 0 (included in EC function) | 0 | 5 |
| ASU | $EC = 22 \cdot \left(\frac{m_{CO_2} [tpd]}{432} \right)^{0.6}$ | 0 (included in EC function) | 0 | 5 |
| Fluidized bed carbonator | $EC = 0.217 \cdot \dot{Q} [MW_h] + 3.83$ | 110% | 20 | 12 |
| Fluidized bed calciner | $EC = 0.193 \cdot (\dot{Q}_{LHV} [MW])^{0.65}$ | 107% | 20 | 12 |
| Entrained flow carbonator | $EC = 85.9 \cdot \left(\dot{V}_{in} \left[\frac{m^3}{s} \right] \right)^{0.5}$ | 0 (included in EC of "Tower structure") | 60 | 12 |
| Entrained flow calciner | $EC = 52.5 \cdot 10^{-3} \cdot \left(\dot{V}_{out} \left[\frac{m^3}{s} \right] \right)^{0.5}$ | 0 (included in EC of "Tower structure") | 60 | 12 |
| Preheater stages (riser, cyclone, feed pipe) | $EC^a = 3.98 \cdot 10^{-9} \cdot (D_{cycl} [mm])^2 + 2.73 \cdot 10^{-6} \cdot D_{cycl} [mm] + 1.6 \cdot 10^{-2}$ | 166% | 0 | 5 |
| Kiln riser | $EC = 8.52 \cdot 10^{-3} \cdot \left(\dot{V}_{out} \left[\frac{m^3}{s} \right] \right)^{0.5}$ | 206% | 0 | 5 |
| Refractory Ducts | $EC = 2.59 \cdot 10^{-2} \cdot \left(\dot{V}_{out} \left[\frac{m^3}{s} \right] \right)^{0.5}$ | 280% | 0 | 5 |
| Insulated Ducts | $EC = 2.44 \cdot 10^{-2} \cdot \left(\dot{V}_{out} \left[\frac{m^3}{s} \right] \right)^{0.5}$ | 240% | 0 | 5 |
| Tower structure | $EC = 35.0 \cdot \frac{M [ton]}{670}$ | 0 (included in EC function) | 25 | 5 |
| Fans | $EC^b = x^c \cdot C_1 \cdot \left(\frac{\dot{V} \left[\frac{m^3}{h} \right]}{V_{ref}} \right)^{0.5} + C_2 \cdot \left(\frac{P [kW]}{P_{ref}} \right)^{0.65}$ | 40% | 0 | 5 |
| Steam turbine | Calculated with (Thermoflow Inc., 2018) | | 0 | 5 |
| Heat exchangers | Calculated with (Thermoflow Inc., 2018) ^d | | 0 ^e | 5 ^e |
| Pumps | Calculated with (Thermoflow Inc., 2018) | | 0 | 5 |
| Feed water preheaters | Calculated with (Thermoflow Inc., 2018) | | 0 | 5 |
| Condenser | Calculated with (Thermoflow Inc., 2018) | | 0 | 5 |
| Cooling Tower | Calculated with (Thermoflow Inc., 2018) | | 0 | 5 |
| CPU | Calculated with (AspenTech, 2016) | | 20 | 12 |

^a Diameter of high efficiency cyclones: $D [mm] = 647 \cdot \dot{V} [m^3/s]^{0.422}$. Diameter of conventional cyclones: $D [mm] = 1,548 \cdot \dot{V} [m^3/s]^{0.28}$.

^b For reference volumetric flow rate $\dot{V}_{ref} = 25,000\text{--}380,000\text{--}485,000\text{ m}^3/\text{h}$; $C_1 = 31.1/254.7/430.5$; for reference power $P_{ref} = 75\text{--}1100\text{--}2000\text{ kW}$; $C_2 = 19.1/148.9/286.6$.

^c Conventional fans: $x = 1$; sealed fans: $x = 1.4$.

^d Material is function of steam temperature: $T < 350\text{ }^\circ\text{C}$: Carbon Steel; $350\text{ }^\circ\text{C} < T < 450\text{ }^\circ\text{C}$: T22; $T > 450\text{ }^\circ\text{C}$: T91. O₂ preheater: stainless steel.

^e Purge cooler: process contingencies factor for maturity and details of equipment list item are 20% and 12% respectively. For O₂ preheater: 5% and 10%.

Table 7
Breakdown of the total plant cost (TPC) of the CaL CO₂ capture plants.

| | Tail-end CaL 20%-IL | Tail-end CaL 50%-IL | Integrated CaL |
|--|---------------------|---------------------|----------------|
| CO₂ capture plant cost, M€ | | | |
| Carbonator | 46.0 | 28.3 | 8.1 |
| Calciner | 23.3 | 19.7 | 9.6 |
| CO ₂ preheater | – | – | 4.6 |
| Kiln gas preheater | – | – | 1.4 |
| Sorbent cooler riser | – | – | 3.7 |
| Kiln risers | | | 0.3 |
| Ducts | | | 2.4 |
| Tower structure | | | 54.8 |
| ASU | 68.9 | 62.5 | 56.9 |
| CPU | 65.4 | 68.0 | 64.0 |
| Fans | 1.9 | 1.7 | 1.3 |
| Limestone grinding plant | 2.2 | 3.8 | – |
| Heat exchangers | 1.7 | 0.7 | 1.2 |
| Steam Turbine | 16.6 | 13.5 | 8.6 |
| Pumps | 0.6 | 0.5 | 0.4 |
| Feed water preheaters and deaerator | 0.7 | 0.5 | 0.4 |
| Condenser | 1.6 | 1.3 | 0.9 |
| Cooling Tower | 2.2 | 1.8 | 1.3 |
| Total CO₂ capture plant cost, M€ | 231.0 | 202.3 | 219.9 |
| Existing cement plant cost, M€ | 203.7 | 203.7 | 203.7 |
| Total plant cost, M€ | 434.7 | 406.0 | 423.6 |

Table 8
Breakdown of the clinker costs for the cement kilns with and without CaL system.

| | Cement kiln w/o CCS | Tail-end 20%-IL CaL | Tail-end 50%-IL CaL | Integrated CaL |
|---|---------------------|---------------------|---------------------|---------------------|
| Raw meal, €/t _{clik} | 5.00 | 4.88 | 4.92 | 5.00 |
| Fuel, €/t _{clik} | 9.41 | 26.16 | 21.30 | 16.31 |
| Electricity, €/t _{clik} | 7.65 | -6.41 | 3.35 | 10.11 |
| Cooling water, €/t _{clik} | 0.00 | 1.15 | 0.85 | 0.64 |
| Other variable costs, €/t _{clik} | 1.74 | 1.74 | 1.74 | 1.74 |
| Variable Opex, €/t_{clik} | 23.79 | 27.52 | 32.16 | 33.79 |
| Labor, €/t _{clik} | 8.93 | 11.29 | 11.23 | 11.32 |
| Insurances and local tax, €/t _{clik} | 4.33 | 9.21 | 8.62 | 9.02 |
| Maintenance cost, €/t _{clik} | 5.41 | 11.51 | 10.78 | 11.28 |
| Fixed Opex, €/t_{clik} | 18.67 | 32.01 | 30.64 | 31.63 |
| Cement kiln, €/t _{clik} | 21.08 | 21.67 | 21.60 | 21.58 |
| CO ₂ capture plant, €/t _{clik} | 0.00 | 24.57 | 21.44 | 23.28 |
| Capex, €/t_{clik} | 21.08 | 46.24 | 43.04 | 44.86 |
| Cost of Clinker/Cement (COC), €/t_{clik} - €/t_{cem} | 63.5 - 46.7 | 105.8 - 77.8 | 105.8 - 77.8 | 110.3 - 81.1 |

Table 9
Breakdown of costs of CO₂ avoided for the different CaL cases assessed.

| | Tail-end 20%-IL CaL | Tail-end 50%-IL CaL | Integrated CaL |
|--|---------------------|---------------------|----------------|
| Fuel, €/t _{CO2} | 20.69 | 14.77 | 8.66 |
| Electricity, €/t _{CO2} | -17.35 | -5.33 | 3.09 |
| Other variable costs, €/t _{CO2} | 1.27 | 0.95 | 0.80 |
| Variable Opex, €/t_{CO2} | 4.61 | 10.39 | 12.54 |
| Fixed Opex, €/t_{CO2} | 16.47 | 14.85 | 16.25 |
| Capex, €/t_{CO2} | 31.05 | 27.26 | 29.82 |
| Cost of CO₂ avoided (CCA), €/t_{CO2} | 52.13 | 52.50 | 58.62 |

CaL reactors (30% and 24% in the 20%- and the 50%-IL cases respectively). The carbonator results to be more expensive than the calciner, because it includes the heat transfer surface to keep the reactor at the target temperature of 650 °C by steam generation. The case with lower integration level (20%-IL) results in a higher Capex, because of the higher amount of fuel burned in the CaL calciner and the consequent

higher cooling duty of the carbonator. After the ASU, the CPU and the CaL reactors, with an overall Capex share of 88% of the CO₂ capture plant, the largest cost in the tail-end CaL plants is associated to the steam turbine (about 7% of the capture plant TPC).

In the integrated CaL case, the carbonator and calciner cost is significantly lower than in the tail-end case (8% of the total CO₂ capture plant cost). The steam turbine also results in a smaller share (4%). On the other hand, the cost of the new tower structure balances out the advantage on the cost of the reactors. The cost of the structure and the related foundations has been assumed to be proportional to the weight of the equipment to be supported. In the integrated CaL case, the weight of the equipment was estimated to be about 1.6 times higher than the weight of the conventional equipment. Therefore, assuming a tower cost of 35 M€ for the reference cement kiln, the cost of the new tower and foundations was estimated to be about 55 M€.

By summing the cost of all the equipment, a total CO₂ capture plant cost of 202 and 231 M€ has been obtained for the 50%-IL and the 20%-IL tail-end plants respectively. For the integrated CaL plant, an intermediate cost of about 220 M€ has been obtained.

The breakdown of the clinker cost is reported in Table 8. Cost of clinker and cement for the reference plant without CO₂ capture is 63.5

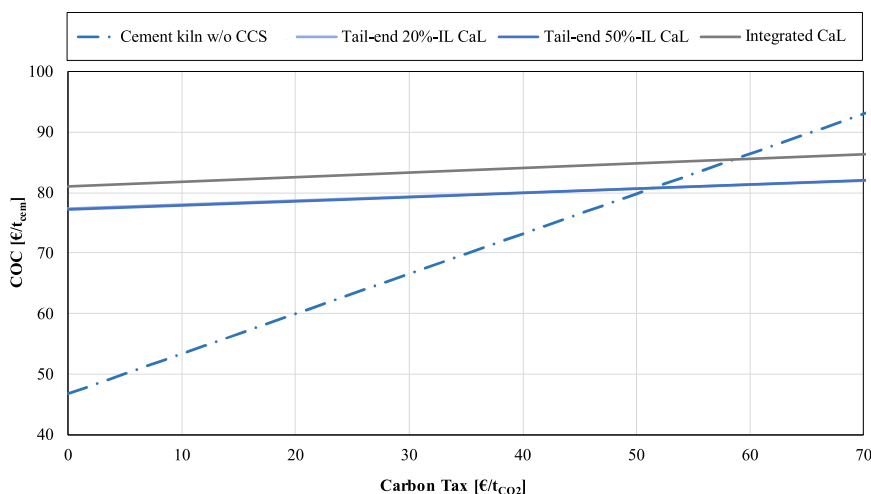


Fig. 8. Cost of cement for the different plants as function of the carbon tax. The two tail-end cases are hardly distinguishable and appear superimposed on this chart.

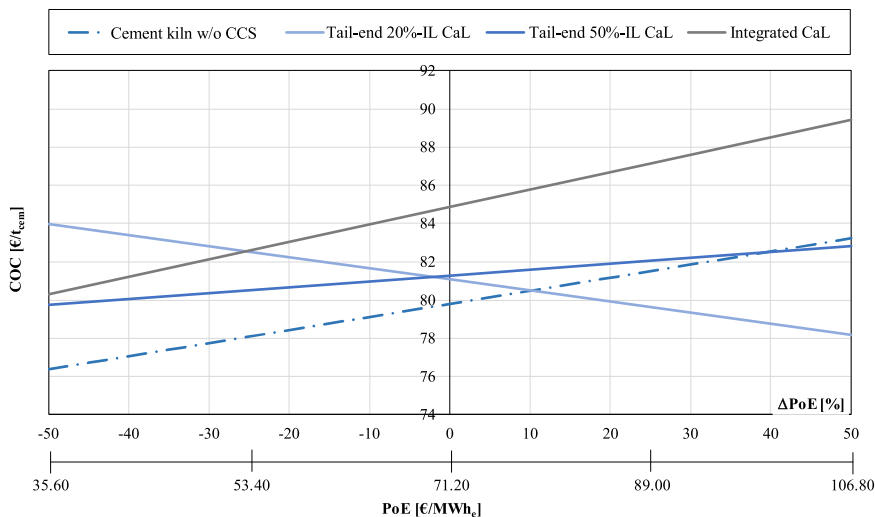


Fig. 9. Cost of cement for the different plants as function of the price of electricity, for a carbon tax of 50 €/t_{CO2}. Note that the reference PoE is increased to 71.2 €/MWh, as it is assumed that the carbon tax affects the electricity price according to its carbon intensity.

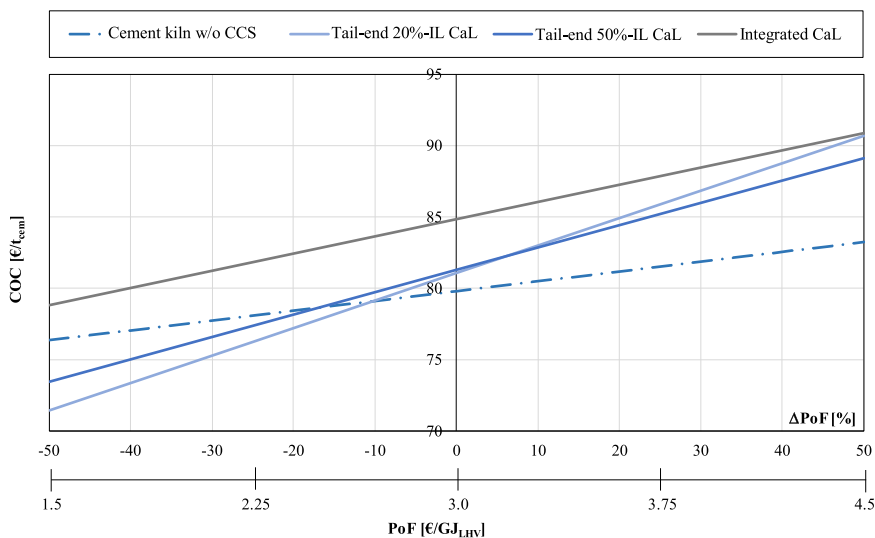


Fig. 10. Cost of cement for the different plants as function of the price of fuel, for a carbon tax of 50 €/t_{CO2}.

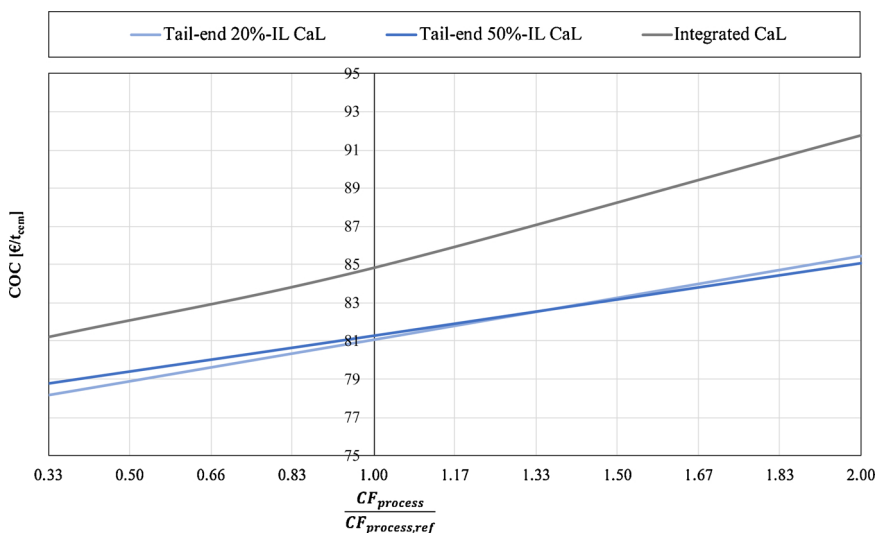


Fig. 11. Cost of cement for the different plants as function of process contingencies, for a carbon tax of 50 €/t_{CO2}.

and 46.7 €/t respectively. Capex, variable Opex and fixed Opex contribute with a similar share to the total cost of clinker. Cost of cement for the CaL plants varies in a relatively narrow range, between 77.4 €/t of the tail-end case with high IL, and 81.1 €/t of the integrated CaL case.

The two tail-end cases show the same cost of cement of 77.8 €/t. The tail-end 20%-IL case is the capture plant with the lowest variable Opex, thanks to the revenues from the net electric power sold to the grid. The lower variable operating costs compensate the higher Capex and fixed Opex, resulting in roughly the same final cost of clinker compared with the tail-end plant with higher IL.

In all the CaL plants, the highest contribution to the cost of clinker derives from the capital expenditures, which are roughly doubled compared to the reference plant. Fixed Opex also increase significantly, being linked to the Capex, as shown in Table 5. Increase of variable costs is also significant and is mainly driven by the cost of fuel.

In Table 9, CO₂ avoided cost breakdown is reported. Total CCA of around 52 €/t have been obtained for the tail-end plants, which is less than the CCA of 58.6 €/t calculated for the integrated CaL plant. In all the cases, the increased Capex are responsible for more than 50% of the total CCA. In the tail-end cases, significant cost is associated to fuel consumption, which is partly compensated by the favorable contribution of the electric balance thanks to the power export (20%-IL) or lower power import (50%-IL) with respect to the reference kiln without capture.

Compared with the techno-economic study by Atsonios et al. (2015), who assessed a tail-end CaL configuration with very low integration level (around 8%), a lower increase of the cost of cement (+67% vs. +84%) and a lower CCA (52 €/t vs. 69 €/t) have been obtained in this work. An economic comparison of the assessed CaL plants with alternative technologies for CO₂ capture in cement plants can be found in (Voldsund et al., 2018), showing that the estimated CCA of CaL processes is higher than oxyfuel technology (42.4 €/t) and lower than post-combustion capture technologies (66.2–83.5 €/t).

In Fig. 8, the sensitivity of the cost of cement on the carbon tax is shown. The dependency of the COC with the carbon tax is much higher in the case without CO₂ capture, reaching more than 90 €/t_{cem} for a carbon tax of 70 €/t_{CO₂}. On the contrary, COC is relatively insensitive to the carbon tax for the plants with CO₂ capture.

In Fig. 9, the sensitivity of the COC on the price of electricity is shown for a carbon tax of 50 €/t_{CO₂}. Negative slope is obtained for the tail-end 20%-IL case, which is a net electricity exporter and therefore benefits from high electricity selling price. COC is negatively affected by higher electricity prices for all the other cases. Nevertheless, a ± 50% variation of the price of electricity leads to a maximum COC variation of ± 5%.

In Fig. 10, the sensitivity of the COC on the price of fuel (PoF) is shown. A variation of the PoF of ± 50% leads to a maximum COC variation of ± 12% (20%-IL tail-end configuration) and a minimum variation of ± 7% (integrated configuration). In general, CaL plants are negatively affected by an increase of the fuel price compared with the reference cement kiln, due to their higher specific fuel consumption.

Finally, in Fig. 11, the sensitivity of the COC on the process contingencies is shown. Process contingencies are varied in the -67%/+100% range compared with the reference contingencies assumed. A similar impact on the COC is obtained for the different systems, namely -5/+8% in integrated case and -3/+5% in the tail-end cases.

5. Conclusions

This work presents the techno-economic comparison of different

Appendix A

Calcium looping processes for CO₂ capture in cement plants. Two CaL technologies have been compared, namely the tail-end CaL process, where fluidized bed CaL reactors treats the flue gas downstream a cement burning process, and the integrated CaL system, where the entrained-flow CaL reactors are integrated in the preheater and the pre-calciner of the cement kiln. The study allows to achieve the following main conclusions.

- Both the CaL plants involves a significant increase of fuel consumption. Such increase is more significant in the tail-end configuration (+119–170%), as the CO₂ released by raw meal calcination and captured in the CaL carbonator requires a second calcination in the oxyfuel CaL calciner. Fuel consumption increase is lower in the assessed integrated CaL process (67%). Both processes allow achieving direct emission reduction between 86.3–90.9% (tail-end cases) and 93.4% (integrated CaL case).
- The additional fuel consumption in the CaL process generate high temperature heat that must be recovered in a steam cycle to generate power. The higher the fuel consumption, the higher the power generated, which make the cement plant a net electricity exporter in the tail-end case with low (20%) integration level (i.e. with low amount of CaCO₃ fed to the CaL system). In the tail-end case with high integration level (50%) and in the integrated CaL plant, power generation allows compensating totally or partially the electricity demand required for oxygen production and CO₂ compression and the cement plant remains a moderate net consumer of electricity.
- Specific primary energy consumption for CO₂ avoided (SPECCA) has been calculated considering the indirect fuel consumptions and CO₂ emissions associated to the electricity imported or exported by the cement plant. Therefore, SPECCA depends on the reference power generation scenario assumed for the electric grid. Depending on the assumed scenario, SPECCA of 3.76–4.42 MJ_{LHV}/kg_{CO₂} for the tail-end cases and of 3.17–3.27 MJ_{LHV}/kg_{CO₂} for the integrated case have been obtained.
- All the CaL technologies are capital intensive. Estimated total plant costs of the capture plant are roughly as high as the cost of the conventional cement plant. In all the cases, more than 50% of the capital cost is associated to the air separation unit and the CO₂ compression and purification unit. In the tail-end CaL cases, a significant cost is also associated to the CaL reactors. In the integrated CaL plant, the highest cost after ASU and CPU is related to the structure of a new tower needed to support the additional equipment of the CaL process components.
- Cost of clinker of 106 €/t_{clk} (+67% compared with the reference case without capture) have been calculated for the tail-end CaL cement plants. A slightly higher value of 110 €/t_{clk} (+74%) have been obtained for the integrated CaL plant. The cost of CO₂ avoided is about 52 €/t_{CO₂} and 58.6 €/t_{CO₂} for the tail-end and the integrated cases respectively.

Acknowledgements

This project has received funding from the European Union's Horizon 2020 research and innovation programme under grant agreement no 641185 (CEMCAP). Mari Voldsund, Stefania Gardarsdottir, Rahul Anantharaman and Simon Roussanaly (SINTEF Energy Research) are also acknowledged for the calculation of the heat and mass balance and the cost of the CPU and for the support in the preparation of the economic model.

References

- Alonso, M., Álvarez Criado, Y., Fernández, J.R., Abanades, C., 2017. CO₂ carrying capacities of cement raw meals in calcium looping systems. *Energy & Fuels* 31, 13955–13962. <https://doi.org/10.1021/acs.energyfuels.7b02586>.
- Anantharaman, R., Berstad, D., Cinti, G., De Lena, E., Gatti, M., Gazzani, M., Hoppe, H., Martínez, I., Monteiro, J., Romano, M., Roussanaly, S., Schols, E., Spinelli, M., Storset, S., van Os, P., Voldsund, M., 2017. CEMCAP Framework for Comparative Techno-economic Analysis of CO₂ Capture from Cement Plants. CEMCAP deliverable D3.2. www.sintef.no/projectweb/cemcap/results/.
- Arias, B., Diego, M.E., Abanades, J.C., Lorenzo, M., Diaz, L., Martínez, D., Alvarez, J., Sánchez-Biezma, A., 2013. Demonstration of steady state CO₂ capture in a 1.7MWth calcium looping pilot. *Int. J. Greenh. Gas Control* 18, 237–245. <https://doi.org/10.1016/j.ijggc.2013.07.014>.
- Arias, B., Alonso, M., Abanades, C., 2017a. CO₂ capture by calcium looping at relevant conditions for cement plants: experimental testing in a 30 kW th pilot plant. *Ind. Eng. Chem. Res.* 56, 2634–2640. <https://doi.org/10.1021/acs.iecr.6b04617>.
- Arias, B., Turrado, S., Alonso, M., Marbán, G., Abanades, C., 2017b. Results of Entrained Flow Carbonator / Calciner Tests. CEMCAP deliverable D12.2. www.sintef.no/projectweb/cemcap/results/.
- AspenTech, 2016. *Aspen One V9.1*.
- Atsonios, K., Grammelis, P., Antiohos, S.K., Nikolopoulos, N., Kakaras, E., 2015. Integration of calcium looping technology in existing cement plant for CO₂ capture: process modeling and technical considerations. *Fuel* 153, 210–223. <https://doi.org/10.1016/j.fuel.2015.02.084>.
- Campanari, S., Cinti, G., Consonni, S., Fleiger, K., Gatti, M., Hoppe, H., Martínez, I., Romano, M., Spinelli, M., Voldsund, M., 2016. Design and Performance of CEMCAP Cement Plant without CO₂ Capture. CEMCAP Deliverable D4.1. www.sintef.no/projectweb/cemcap/results/.
- CEMCAP, 2015. EU H2020 Project: CO₂ Capture from Cement Production. Grant Agreement n.641185. www.sintef.no/cemcap/.
- Cinti, G., Anantharaman, R., De Lena, E., Fu, C., Gardarsdottir, S.O., Hoppe, H., Jamali, A., Romano, M., Roussanaly, S., Spinelli, M., Stallmann, O., Voldsund, M., 2018. Cost of Critical Components in CO₂ Capture Processes. CEMCAP deliverable D4.4. www.sintef.no/projectweb/cemcap/results/.
- Consonni, S., Viganò, F., 2012. Waste gasification vs. Conventional Waste-To-Energy: a comparative evaluation of two commercial technologies. *Waste Manag.* 32, 653–666. <https://doi.org/10.1016/j.wasman.2011.12.019>.
- De Lena, E., Spinelli, M., Martínez, I., Gatti, M., Scaccabarozzi, R., Cinti, G., Romano, M.C., 2017. Process integration study of tail-end Ca-Looping process for CO₂ capture in cement plants. *Int. J. Greenh. Gas Control* 67, 71–92. <https://doi.org/10.1016/j.ijggc.2017.10.005>.
- De Lena, E., Spinelli, M., Romano, M.C., Voldsund, M., Gardarsdottir, S.O., Roussanaly, S., 2018. CEMCAP Economic Model Spreadsheet. Annex of CEMCAP deliverable D4.6. www.sintef.no/projectweb/cemcap/results/.
- GECOS, 2016. GS Software. www.gecos.polimi.it.
- Geldart, D., 1973. Types of gas fluidization. *Powder Technol.* 7. [https://doi.org/10.1016/0032-5910\(73\)80037-3](https://doi.org/10.1016/0032-5910(73)80037-3).
- Hornberger, M., Spörl, R., Scheffknecht, G., 2017. Calcium looping for CO₂ capture in cement plants – pilot scale test. *Energy Procedia* 114, 6171–6174. <https://doi.org/10.1016/j.egypro.2017.03.1754>.
- IEA, 2017. Energy Technology Perspectives 2017. OECD https://doi.org/10.1787/energy_tech-2017-en.
- Jamali, A., Fleiger, K., Ruppert, J., Hoenig, V., Anantharaman, R., 2018. Optimised Operation of an Oxyfuel Cement Plant. CEMCAP Deliverable D6.1. www.sintef.no/projectweb/cemcap/results/.
- Kremer, J., Galloy, A., Ströhle, J., Epple, B., 2013. Continuous CO₂ capture in a 1-MWth carbonate looping pilot plant. *Chem. Eng. Technol.* 36, 1518–1524. <https://doi.org/10.1002/ceat.201300084>.
- Marchi, M.I., Cinti, G., Romano, M.C., Campanari, S., Consonni, S., 2012a. Improved Process for the Production of Cement Clinker and Related Apparatus (in Italian). Patent application MI2012 A00382. .
- Marchi, M.I., Cinti, G., Romano, M.C., Campanari, S., Consonni, S., 2012b. Process and Improved Plant for the Production of Cement Clinker (in Italian). Patent application MI2012 A00383. .
- NETL, 2012. Quality Guidelines for Energy System Studies - CO₂ Impurity Design Parameters. DOE/ NETL-341/011212. .
- Olivier, J.G.J., Janssens-Maenhout, G., Muntean, M., Peters, J.A.H.W., 2016. Trends in Global CO₂ Emissions: 2016 Report, The Hague: Pbl CO₂ Netherlands Environmental Assessment Agency; Ispra: European Commission. Joint Research Centre.
- Ozcan, D.C., Ahn, H., Brandani, S., 2013. Process integration of a Ca-looping carbon capture process in a cement plant. *Int. J. Greenh. Gas Control* 19, 530–540. <https://doi.org/10.1016/j.ijggc.2013.10.009>.
- Pathi, S.K., Lin, W., Illerup, J.B., Dam-Johansen, K., Hjuler, K., 2013. CO₂ capture by cement raw meal. *Energy and Fuels* 27, 5397–5406. <https://doi.org/10.1021/ef401073p>.
- Rodríguez, N., Murillo, R., Abanades, J.C., 2012. CO₂ capture from cement plants using oxyfired precalcination and/ or calcium looping. *Environ. Sci. Technol.* 46, 2460–2466. <https://doi.org/10.1021/es2030593>.
- Romano, M.C., 2012. Modeling the carbonator of a Ca-looping process for CO₂ capture from power plant flue gas. *Chem. Eng. Sci.* 69, 257–269. <https://doi.org/10.1016/j.ces.2011.10.041>.
- Romano, M.C., Spinelli, M., Campanari, S., Consonni, S., Marchi, M., Pimpinelli, N., Cinti, G., 2014. The calcium looping process for low CO₂ emission cement plants. *Energy Procedia* 61, 500–503. <https://doi.org/10.1016/j.egypro.2014.11.1158>.
- Spinelli, M., Martínez, I., De Lena, E., Cinti, G., Hornberger, M., Spörl, R., Abanades, J.C., Becker, S., Mathai, R., Fleiger, K., Hoenig, V., Gatti, M., Scaccabarozzi, R., Campanari, S., Consonni, S., Romano, M.C., 2017. Integration of Ca-Looping systems for CO₂ capture in cement plants. *Energy Procedia* 114, 6206–6214. <https://doi.org/10.1016/j.egypro.2017.03.1758>.
- Spinelli, M., Martínez, I., Romano, M.C., 2018. One-dimensional model of entrained-flow carbonator for CO₂ capture in cement kilns by Calcium looping process. *Chem. Eng. Sci.* 191, 100–114. <https://doi.org/10.1016/j.ces.2018.06.051>.
- ThermoFlow Inc, 2018. Thermoflex v.27.0. www.thermoflow.com.
- Turrado, S., Arias, B., Fernández, J.R., Abanades, J.C., 2018. Carbonation of fine CaO particles in a drop tube reactor. *Ind. Eng. Chem. Res.* 57, 13372–13380. <https://doi.org/10.1021/acs.iecr.8b02918>.
- Voldsund, M., Anantharaman, R., Berstad, D., De Lena, E., Fu, C., Gardarsdottir, S.O., Jamali, A., Pérez-Calvo, J.-F., Romano, M., Roussanaly, S., Ruppert, J., Stallmann, O., Sutter, D., 2018. CEMCAP Comparative Techno-economic Analysis of CO₂ Capture in Cement Plants. CEMCAP deliverable D4.6. www.sintef.no/projectweb/cemcap/results/.